Malaya Journal of Matematik, Vol. 8, No. 2, 668-673, 2020

https://doi.org/10.26637/MJM0802/0059

Mass transfer phenomena of MHD nanofluid with chemical reaction with base fluids water and kerosene

K. Saritha[1]*, T. Gandhimathi[2] and M. Rameshkumar[3]

Abstract

Mass Transfer of MHD nanofluid flow phenomena with chemical reaction and prescribed mass flux is analyzed. This work is composed of 5 nanoparticles such as Cu,Ag,Al,Al_2O_3 and TiO_2 and two base fluids water and kerosene . Momentum and concentration equations are solved using the Runge-Kutta-Fehlberg method of numerical technique. The flow analysis and concentration of nanofluid Cu-water and Cu-kerosene by the effect of magnetic parameter, nanoparticle volume fraction, permeability parameter, suction parameter, Schmidt number and chemical reaction parameter is analyzed. The Sherwood number of various nanofluids are tabulated and analyzed. Comparison analysis was performed with the data recorded previously. It is concluded that the rate of mass transfer of kerosene based nanofluids is lower than that of water based nanofluids.

Keywords

Porous surface; Nanofluid; Water and Kerosene Chemical reaction; Mass flux.

AMS Subject Classification:76D05,76D55, 76W05, 76S05, 76R10.

[1,2,3] *Department of Mathematics, P.A College of Engineering and Technology, Pollachi-642002, Tamil Nadu, India.*

***Corresponding author**: [1] sarimathspacet@gmail.com

Article History: Received **12** January **2020**; Accepted **18** April **2020**

Contents

1. Introduction

The mass transfer process has some of the most defining problems in chemical engineering. A unique characteristic of a chemical engineer is his ability to build and operate an equipment in which the components are prepared for reaction. The resulting product separation is established as a result of reactions. This skill is largely focused on the know- mass transfer science. Applications of the concepts of momentum and heat transfer are widespread in many engineering fields, but historically, the application of mass transfer has been mainly limited to chemical engineering. Many important applications exist in metallurgical processes and in the construction of high-speed aircraft, more recently.

Xie et. al. [15] examined nanofluids that contain multi-walled carbon nanotubes and their enhanced thermal conductivities. Olle et. al. [8] used functionalized magnetic nanoparticles to analyze the enhancement of the oxygen mass transfer. Nagy et. al. [7] investigated the enhancement of oxygen mass transmission rate in the presence of nanosized particles. Komatiand Suresh [14] investigated the enhancement of mass transfer using nano-magentic iron-oxide particles. Mass transfer in nanofluids was reviewed by Seyedeh et. al. [12]. Khanolkar and Suresh [5] performed experiments and simulations for improved nanofluid mass transfer speeds. Singh and Kumar has investigated the mass transfer of alumina water nanofluid in MHD flow over a flat plate under slip conditions. Khilap and Kumar [6] are researching mass transfer of a micropolar fluid flow in a permeable manner with the effects of the chemical reaction system. Dhuria et. al. [11] investigated diffusiophoretic enhancement of nanofluid mass transfer. Wissink et. al. (2017) investigated the effect of surface contamination on the rate of mass transfer of low diffusivity gas across a flat surface using direct numerical simulations. Tolesorkhietal [13] did experimental and theo-

retical investigation of CO2 mass transfer enhancement of silica nanoparticles in water. Venuta et. al. (2018) studied the computational simulation of the mass transfer and the fluid flow evolution of a rectangular free air stream. Cay et. al. [2] investigated the simulation of the CFD heat pipe in NH3-water nanofluid flow.

So far, in the presence of defined mass flux, no major contribution has been made to the mass transfer of nanofluid flow with chemical reaction. In this function, consideration is given to nano fluids with nanoparticles Cu, Ag, Au, Al, Al_2O_3 and TiO_2 and water and kerosene with the base fluids. The equations governing system is numerically solved. Using diagrams, the effect of various physical parameters on the species concentration of nanofluid Cu-water and Cu-kerosene nanofluids is analyzed. The Sherwood number of specific nanofluids with nanoparticles Cu, Ag, Al, Al_2O_3 and TiO_2 is tabulated and analyzed.

2. Formulation of the problem

Mass transfer analyzes are formulated in a Nanofluid's boundary layer flow with chemical reaction and magnetic effect. Consideration is provided to two types of base fluids (water and kerosene) and five types of nanoparticles (Cu, Ag, Al, Al_2O_3 and TiO_2). Porous surface with defined mass flux is known as the conditions of surface boundary. The components of velocity u and v are taken along the directions x and y respectively. The problem's governing equations with boundary conditions are as

$$\frac{\partial u}{\partial x}+\frac{\partial v}{\partial y}=0 \tag{2.1}$$

$$u\frac{\partial u}{\partial x}+v\frac{\partial u}{\partial y}=\nu_{nf}\frac{\partial^2 u}{\partial y^2}-\frac{\nu_{nf}}{K_p}u-\frac{\sigma B_0^2 u}{\rho_{nf}} \tag{2.2}$$

$$u\frac{\partial C}{\partial x}+v\frac{\partial C}{\partial y}=D\frac{\partial^2 C}{\partial y^2}-k_1(C-C_\infty) \tag{2.3}$$

where

$$\mu_{nf}=\frac{\mu_f}{(1-\phi)^{2.5}}, \nu_{nf}=\frac{\mu_{nf}}{\rho_{nf}}$$

$$\rho_{nf}=(1-\phi)\rho_f+\phi\rho_s,$$

The conditions of the boundary are

$$u=ax, v=-V_0 \quad at \quad y=0$$

$$-D\frac{\partial C}{\partial y}=m_w=E_1x^2 \quad at \quad y=0$$

$$u=0 \quad C\to C_\infty \quad as \quad y\to\infty \tag{2.4}$$

Suitable similarity transformations are implemented to transform equations 2.1 – 2.3 into the non linear ordinary differential equations as

$$\psi=\left(av_f\right)^{0.5}xf(\eta), \eta=y\left(\frac{a}{v_f}\right)^{0.5}, u=\frac{\partial\psi}{\partial y}, \\ v=-\frac{\partial\psi}{\partial x}, C-C_\infty=\frac{E_1x^2}{D}\sqrt{\frac{v_f}{a}}h(\eta) \tag{2.5}$$

The equations are given by

$$f'''+\phi_1\left(ff''-f'^2\right)-\left(\frac{1}{R_p}+\frac{M^2}{\phi_2}\right)f'=0 \tag{2.6}$$

$$h''+S_cfh'-2S_cfh'-\gamma S_ch=0 \tag{2.7}$$

$$f'(\eta)=1 \quad f(\eta)=S \quad h'(\eta)=-1 \quad at \quad \eta=0 \\ f'(\eta)=0 \quad h(\eta)=0 \quad as \quad \eta\to\infty \tag{2.8}$$

$$\phi_1=(1-\phi)^{2.5}\left[(1-\phi)+\phi\frac{(\rho)_s}{(\rho)_f}\right] \phi_2=(1-\phi)+\phi\frac{(\rho)_s}{(\rho)_f}$$

	Density $\rho(kg/m^3)$	Specific heat $C_p(J/kgK)$	Thermal conductivity $K(W/mK)$
Water	997.1	4179	0.613
Kerosene	783	2090	0.145
Copper(Cu)	8933	385	401
Silver(Ag)	10500	235	429
Aluminum(Al)	2710	913	201
Aluminum Oxide (Al_2O_3)	3970	765	40
Titanium Oxide (TiO_2)	4250	686.2	8.9538

Table 1. Physical Properties of Water and Nanoparticles Palaniammal and Saritha (2017)

$R_p=\frac{K_pa}{v_f}$(Permeability Parameter),$\gamma=\frac{K_1}{a}$ (Chemical reaction parameter), $s_c=\frac{v_f}{D}$(Schmidt number), $S=\frac{V_0}{\sqrt{v_fd}}$(Suction parameter), $M=\frac{\sigma B_0^2}{a(\rho)_f}$(Magnetic Parameter), D is mass diffusivity, k_1 is chemical reaction constant and E_1 is constant. The Sherwood number represents rate mass transfer which is given by using similarity transformation

$$sh=\frac{m_wx}{D(C-C_\infty)}=\frac{1}{h(0)} \tag{2.9}$$

3. Numerical Solution

Equations 2.6-2.7 are strongly nonlinear simultaneous ordinary differential equations for different values of specific

parameters are solved with the aid of the shooting method in accordance with the Runge-Kutta-Fehlberg technique. Therefore, initially governing equations are converted into differential equations of first order, and good initial approximations are chosen.

4. Results and Discussion

The physical significance of the flow area, concentration is evaluated and results are shown graphically, typical values of different physical parameters such as Magnetic parameter M, nanoparticle volume fraction ϕ, Permeability parameter R_p, Suction parameter S, Schmidt number S_c and Chemical reaction parameter π in the case of Cu-Water / Kerosene nanofluid. Sherwood number is also tabulated in specified nanofluids. The thermo-physical properties of the base fluids and nanoparticles $(Cu, Ag, Al, Al_2O_3$ and $TiO_2)$ are described in Table 1.

M	Anjali Devi et al(2013)	Present work
0	0.676774	0.67677428
1	0.697755	0.69775508
4	0.737861	0.73786087
9	0.776667	0.77666685
16	0.809680	0.80967977

Table 2. Comparison of $h(0)$ with the previous reported work $(S = 1.5, R_p = 100, S_c = 0.62, \varphi = 0, \gamma = 0)$

Comparison analysis to verify the consistency of the findings with the previously reported data is performed through Table 2. In a few special cases, the present findings of $h(0)$ are found to be an outstanding agreement with the research published previously. Figure 1 shows the influence of magnetic field on the Cu-water and Cu-kerosene nanofluid concentration profiles. It is represented that the magnetic field strengthening induces the opposite force to the flow. This force has the tendency of increasing the fiction between the layers of concentration. Therefore the result of an increase in M is to increase the concentration. Cu-water concentrations are also found to be higher than Cu-kerosene.

Figure 2 demonstrates the effect of the fraction of nanoparticles on the concentration profiles. In both Cu-water and Cu-kerosene cases it is observed that the effect of the volume fraction of nanoparticles is decreases the concentration. The presence of solid nanoparticles reduces the thickness of the boundary layer concentration and also points out that Cu-water concentration is lower than Cu-Kerosene.

The effect of Permeability Parameter R_p on concentration is seen in Figure 3. It is known that the increase in R_p results in a reduction in the distribution of species concentration for both Cu-water and Cu-kerosene nanofluids. The porous medium is increased by permeability which allows the fluid to pass freely through the boundary layer. This leads to an increase in the area of boundary layer concentration. Cu-water nanofluid is found to have higher concentrations than Cu-kerosene.

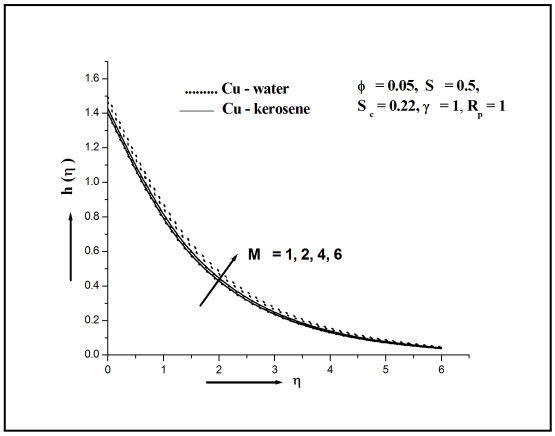

Figure 1. Concentration profiles for M

The impact of suction parameter S on the distribution of Cu-water and Cu-kerosene in species concentrations is shown in Figure 4. In both cases the effect of S on concentration is considered to be reduced. The fluid is pushed closer to the porous surface while increasing the suction parameter. This allows the thickness of the boundary layer of concentration to decrease. The concentration of Cu-water nanofluid is also found to be higher than that of Cu-kerosene.

Figure 5 shows the influence of the Schmidt number Sc on Cu-water and Cu-kerosene nanofluid concentration profiles of the organisms. In both fluids, concentration is shown to diminish with Sc values. Schmidt number is a ratio of diffusive momentum to diffusivity of the mass. As the increase in the amount of Schmidt reduces the mass diffusivity, the thickness of the boundary layer of concentration is reduced. Cu-water nanofluid concentration is comparatively higher than Cu-kerosene.

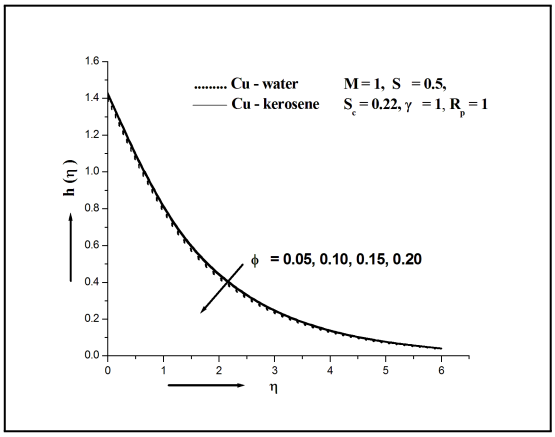

Figure 2. Concentration profiles for ϕ

Figure 6 shows the effect of the chemical reaction parameter γ on the distribution of Cu-water and Cu-kerosene nanofluids concentration of species. When γ increases, the concentration for both fluids decreases. It is due to the increased chemical reaction rate within the solution, which

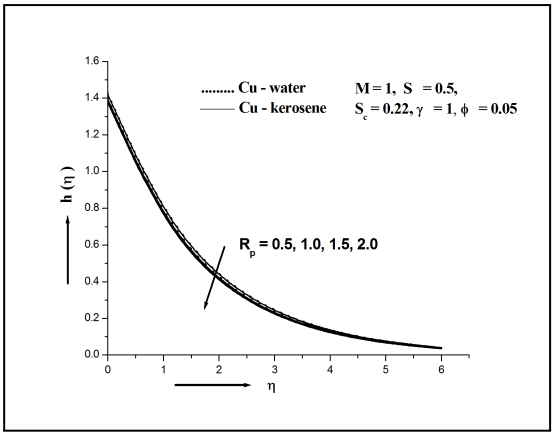

Figure 3. Concentration profiles for R_p

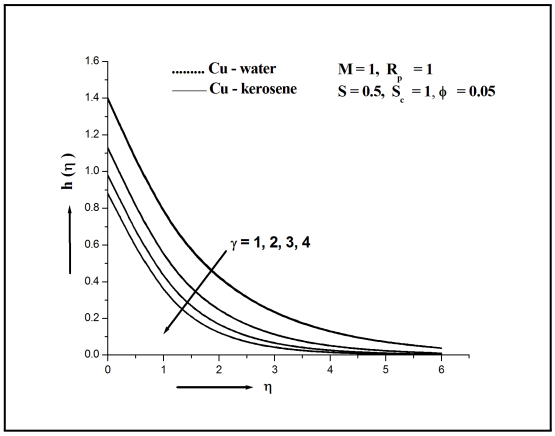

Figure 6. Concentration profiles for γ

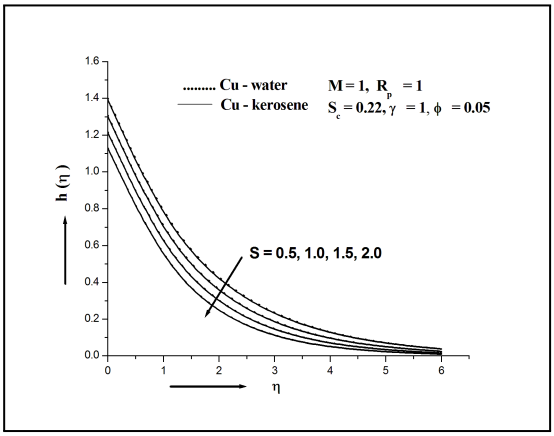

Figure 4. Concentration profiles for S

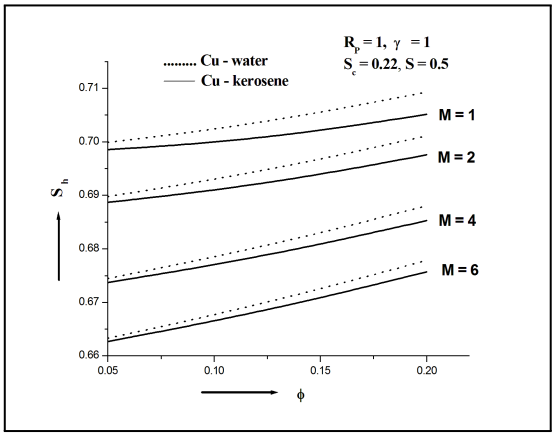

Figure 7. Sherwood Number for M

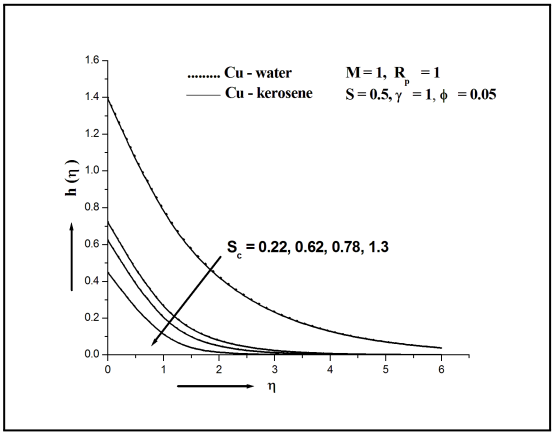

Figure 5. Concentration profiles for S_c

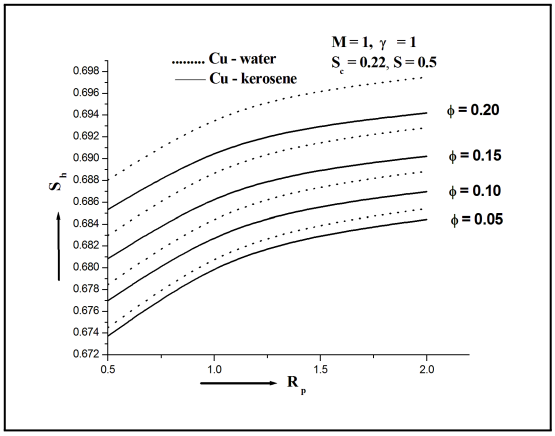

Figure 8. Sherwood Number for ϕ

allows the concentration to reduce.

Figures 7- 9 show the Sherwood number of different values ofM, φ and S of Cu-water and Cu-kerosene nanofluids. It is noted that the Sherwood number increases while the values of φ and S increase as it decreases with the increase of M. The mass transfer rate rises with an rise in the value of φ and S, and decreases with a rise in M. The amount of Cu-water nanofluid in Sherwood number is higher than the nanofluid in Cu-kerosene.

Table 3 displays the values of the Sherwood number of specific nanofluids with the $Ag, Al, Al_2O_3 and TiO_2$ nanoparticles and the water and kerosene base fluids for enhanced

	SILVER			ALUMINIUM			ALUMINIUM OXIDE			TITANIUM OXIDE		
WATER BASED NANOFLUID												
ϕ	S=0.5	M=1.0	R_p=0.5	S=0.5	M=1.0	R_p=0.5	S=0.5	M=1.0	R_p=0.5	S=0.5	M=1.0	R_p=0.5
0.05	0.68088	0.69900	0.67399	0.68389	0.70354	0.67655	0.68339	0.70277	0.67613	0.68328	0.70260	0.67604
0.1	0.68399	0.70069	0.67750	0.68981	0.70924	0.68248	0.68882	0.70775	0.68164	0.68860	0.70742	0.68145
0.15	0.68773	0.70322	0.68158	0.69618	0.71535	0.68887	0.69890	0.71317	0.68761	0.69438	0.71270	0.68733
0.2	0.69211	0.70658	0.68627	0.70302	0.72190	0.69576	0.70108	0.71909	0.69409	0.70066	0.71848	0.69372
	S=1.0	M=2.0	R_p=1.0	S=1.0	M=2.0	R_p=1.0	S=1.0	M=2.0	R_p=1.0	S=1.0	M=2.0	R_p=1.0
0.05	0.73661	0.68905	0.68088	0.73919	0.69268	0.68389	0.73876	0.69208	0.68339	0.73867	0.69194	0.68328
0.1	0.73927	0.69159	0.68399	0.74424	0.69854	0.68981	0.74339	0.69734	0.68882	0.74321	0.69708	0.68860
0.15	0.74246	0.69484	0.68773	0.74961	0.70483	0.69618	0.74837	0.70306	0.69890	0.74810	0.70268	0.69438
0.2	0.74619	0.69880	0.69211	0.75533	0.71158	0.70302	0.75371	0.70927	0.70108	0.75336	0.70877	0.70066
KEROSENE BASED NANOFLUID												
ϕ	S=0.5	M=1.0	R_p=0.5	S=0.5	M=0	R_p=0.5	S=0.5	M=0	R_p=0.5	S=0.5	M=0	R_p=0.5
0.05	0.67982	0.69743	0.67309	0.68360	0.70308	0.67630	0.68632	0.70212	0.67577	0.68282	0.70191	0.67565
0.1	0.68202	0.69788	0.67580	0.68923	0.70835	0.68199	0.68798	0.70650	0.68092	0.68771	0.70610	0.68069
0.15	0.68497	0.69942	0.67917	0.69530	0.71406	0.68813	0.69347	0.71138	0.68655	0.69307	0.71080	0.68621
0.2	0.68866	0.70195	0.68322	0.70187	0.72023	0.69477	0.69947	0.71678	0.69269	0.69895	0.71604	0.69224
	S=1.0	M=2.0	R_p=1.0	S=1.0	M=1.0	R_p=1.0	S=1.0	M=1.0	R_p=1.0	S=1.0	M=1.0	R_p=1.0
0.05	0.73570	0.68777	0.67982	0.73894	0.69232	0.68360	0.73840	0.69156	0.68632	0.73828	0.69139	0.68282
0.1	0.73759	0.68927	0.68202	0.74374	0.69783	0.68923	0.74268	0.69634	0.68798	0.74245	0.69601	0.68771
0.15	0.74011	0.69163	0.68497	0.74887	0.70378	0.69530	0.74733	0.70159	0.69347	0.74699	0.70112	0.69307
0.2	0.74326	0.69484	0.68866	0.75437	0.71021	0.70187	0.75237	0.70737	0.69947	0.75193	0.70676	0.69895

Table 3. Sherwood numbers of various Nanofluids

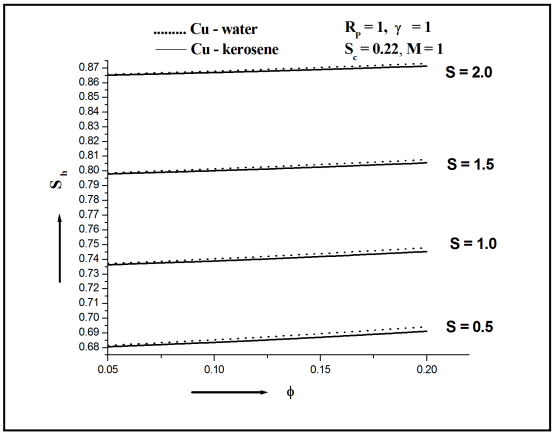

Figure 9. Sherwood Number for S

values of parameters M, φ and S. It is observed that the Sherwood number increases with the increase of φ and S but the effect of M decreases the Sherwood number. It is also noted that Sherwood number of nanofluids with base fluid water is comparatively higher than that of kerosene nanofluids.

5. Conclusion

The flow of MHD nanofluid with Cu, Ag, Al, Al_2O_3, and TiO_2 nanoparticles and water and kerosene with the base fluids is analyzed. This paper performed mass transfer with chemical reaction subject to prescribed mass flux. In general, all the physical parameters influence the distribution of the Cu-water and Cu-kerosene nano fluids species concentration.

The distribution of the species concentration increases with an increase in magnetic parameter value and decreases with the values of the suction parameter, nanoparticle volume fraction fraction, permeability parameter, Schmidt number and chemical reaction parameter.

The Sherwood number of nanofluids with the Cu, Ag, Al, Al_2O_3andTiO_2 nanoparticles and with the water and kerosene base fluids is analyzed for various magnetic parameter, volume fraction of nanoparticles and suction parameter.

It is concluded that the rate of mass transfer of kerosene based nanofluids is lower than that of water based nanofluids.

References

[1] S.P. Devi and M. Kayalvizhi, Nonlinear hydro magnetic flow with radiation and heat source over a stretching surface with prescribed heat and mass flux embedded in a porous medium, *Journal of Applied Fluid Dynamics,* 6(2)(2013), 157-165.

[2] Y. Çay, Mortaşa TN and Çalışkanba FCFD heat pipe simulation of mass transferin NH_3-water nanofluid flow , *Acta Physica Polonica,* 134, 2018, 1–10.

[3] Ivan Di Venuta, Ivano Petracci, Matteo Angelino, Andrea Boghi and Fabio Gori, Numerical simulation of mass transfer and fluid flow evolution of a rectangular free jet of air, *International Journal of Heat and Mass Transfer,* 117(2018), 235-251.

[4] Jan Gerard Wissink, Herlina, Herlina, Yasemin Akar and Markus Uhlmann, Effect of surface contamination on interfacial mass transfer rate, *Journal of Fluid Mechanics,* 830(2017), 5-34.

[5] Khanolkar U Ratnesh, Suresh AK, Enhanced mass transfer rates in nanofluids: experiments and modeling, *Journal of Heat Transfer,* 137(2015), 1–10.

[6] Khilap Singh and Manoj Kumar, Influence of chemical reaction on heat and mass transfer flow of a micropolar fluid over a permeable channel with radiation and heat generation, *Journal of Thermodynamics,* Volume 2016, Article ID 8307980.

[7] Nagy E, Feczkó T and Koroknai B, Enhancement of oxygen mass transfer rate in the presence of nano-sized particles, *Chemical Engineering Science,* 62(2007), 7391–7398.

[8] Olle, B Bucak S, Holmes T C, Bromberg, L, Hatton T A and Wang, DIC, Enhancement of oxygen mass transfer using functionalized magnetic nanoparticles, *Industrial and Engineering Chemistry Research,* 45(2006), 4355–4363.

[9] Padam Singh and Manoj Kumar, Mass transfer in MHD flow of alumina water nanofluid over a flat plate under slip conditions, *Alexandria Engineering Journal,* 54(2015), 383–387.

[10] Palaniammal S P and Saritha K, Heat and mass transfer of a casson nanofluid flow over a porous surface with dissipation, radiation, and chemical reaction. *IEEE Transactions on Nanotechnology,* 16(2017), 909-917.

[11] Rakhi Dhuriya, Varun Dalia and Sunthar P, Diffusiophoretic enhancement of mass transfer by nanofluids, *Chemical Engineering Science,* 176(2006), 632 – 640.

[12] Sanjib Sengupta, Nazibuddin Ahmed, Seyedeh-Saba Ashrafmansouri and Mohsen Nasr Esfahany, Mass transfer in nanofluids, *A review International Journal of Thermal Sciences,* 82(2014), 84–99.

[13] Soosan Farzani Tolesorkhi, Feridun Esmaeilzadeh and Masoud Riazi, Experimental and theoretical investigation of CO2 mass transfer enhancement of silica nanoparticles in water, 3(2018), 370–380.

[14] Srinivas Komati and Akkihebbal K. Suresh, Anomalous enhancement of interphase transport rates by nanoparticles effect of magnetic iron oxide on gas−liquid mass transfer,*Industrial and Engineering Chemistry Research,* 49(2010), 390–405.

[15] Xie H, Lee H, Youn W and Choi M, Nanofluids containing multiwalled carbon nanotubes and their enhanced thermal conductivities, *Journal of Applied Physics,* 94(2003), 4967–4971.

⋆⋆⋆⋆⋆⋆⋆⋆⋆

ISSN(P):2319 – 3786

Malaya Journal of Matematik

ISSN(O):2321 – 5666

⋆⋆⋆⋆⋆⋆⋆⋆⋆